International Journal of Applied Science and Engineering
2013. 11, 3: 277-292

ANSYS Based FEM Analysis for Three and Four Coil Active Magnetic Bearing-a Comparative Study

Pabitra Kumar Biswas [a,*] and Subrata Banerjee [b]

[a] *Department of Electrical Engineering, Asansol Engg. College, Asanso, West Bengal, India*
[b] *Department of Electrical Engineering, National Institute of Technology, Durgapur, West Bengal, India*

Abstract: The active magnetic bearing (AMB) is an integral part of the industrial rotational machine. The paper deals with simulation study of three and four coil AMB utilizing Finite Element Method (FEM). This paper also presents how ANSYS software (Ver. 12.1) can be used to perform the magnetic field analysis in the AMB. This work reports ANSYS simulation for two different structure of AMB that uses three and four attraction type magnets placed in 120 and 90 degree apart from each and other respectively. Three and four attractive magnets give an unstable static force, decreasing with greater distance, and increasing at close distances between electromagnet (stator) and rotor. The nonlinear solution of the magnetic vector potential is determined by using the 2-D finite element method. The force is calculated by Maxwell's stress tensor method. The electromagnetic field distribution and density analysis allow verifying the designed AMB and the influence of the shaft and coil current changes on the bearing parameters.

Keywords: Electromagnetic field; active magnetic bearing; finite element method; ANSYS software; flux pattern.

1. Introduction

Magnetic bearings are electromagnetic actuators. They work according to electromagnetic principle, which says that a magnetic field is induced by moving charges. The magnetic field excites reluctance forces at boundaries of material with different magnetic permeabilities. Active magnetic bearing (AMB) is a new kind of bearing. Unlike conventional bearings, which rely on mechanical forces originating from fluid films or physical contact to support bearing loads, AMB systems utilize controllable electromagnetic force caused by electromagnet to levitate and support a shaft in an air-gap between the bearing stators [1]. AMB offer the following unique advantages: non-contact, friction-less, high speed, low power loss, high accuracy, elimination of lubrication and so on. Due to these advantages, AMB is used widely in many fields such as transportation, high-speed machine tool, aerospace, precision instrumentation etc [2]. A magnetic bearing is a bearing which supports a load using magnetic levitation. Magnetic bearings support moving machinery without physical contact, for example, they can levitate a rotating shaft and permit relative motion without friction or wear. They are in service in such industrial applications as electric power generation, petroleum refining, machine tool operation and natural gas pipelines. Magnetic bearings support the highest speeds of any kind of bearing, it have no

* Corresponding author; e-mail: pabitra.biswas2009@gmail.com

Received 29 June 2012
Revised 21 November 2012
Accepted 7 March 2013

known maximum relative speed. It is difficult to build a magnetic bearing using permanent magnets due to the limitations described by Earns haw's theorem, and techniques using diamagnetic materials are relatively undeveloped. As a result, most magnetic bearings require continuous power input and an active control system to hold the load stable. Because of this complexity, the magnetic bearings also typically require some kind of back-up bearing in case of power or control system failure [2, 4]. For rotating systems it is possible to use homopolar magnet designs instead of multipole halbach structures, which reduces losses considerably [3, 4]. The finite-element method can be a tool for magnetic field analysis of AMB systems.

Figure 1 shows the basic block diagram of the single-axis active magnetic bearing with different components. It appears that AMB essentially consists of an electromagnet, power amplifier, controller, and gap sensor. A magnetic rotor is suspended by an electromagnet. In order to get an active control of the rotor, its position is measured by a position sensor. The position signal is then treated by a controller, which gives a current set point. This signal is then amplified by the power amplifier, in order to get the necessary actuator current. The power amplifiers in a modern commercial application are solid state devices which operate in a pulse width modulation (PWM) configuration [1, 2]. A closed loop control is thus realized and the system can be stabilized. This single actuator enables the levitation along only one axis and only in one direction. In AMB systems, several actuators are used in order to control the rotor levitation along several degrees-of-freedom (DOF). Actuators are typically arranged as pairs facing each-other. This enables to attract the rotor in two opposite directions along one axis. The power amplifiers supply equal bias current to two pairs of electromagnets on opposite sides of a rotor. The gap sensors are usually inductive in nature and sense in a differential mode.

FEMLAB software applied to active magnetic bearing analysis by A. Pilat [1] gives an overall idea of 2-D FEM analysis of active magnetic bearing using COMSOL. A simplified, two dimensional model of the AMB is considered where effects associated with stator and shaft lengths are omitted [2]. Using the COMSOL feature that allows measuring field properties at the defined point the magnetic potential has measured at different rotor displacements. A. Pilat etal [2] has stated that calculations based on the finite element method give a deeper insight into the design of AMB. (T. Ludvig and M. Kuczmann) [4] has analyzed AMB system by finite element method that is based on magnetic vector potential.

The hetero-polar LWG-type Active Magnetic Bearing was analyzed in (Gosiewski and Falkowski, 2003), with the discussion of magnetic field properties at the desired current level and numerical aspects. The finite-element method was also used to analyze the air gap flux and radial forces in miniature self bearing motors (Kim S., Masuzawa T and Okada, 2002; Ohmori et al., 2002) [6]. The control algorithms as well as the motion dynamics are implemented directly in the COMSOL Multiphysics.The nonlinear solution of the magnetic vector potential is determined, using the 2D finite element method. The force is calculated by Maxwell's stress tensor method [13].

In this work two-dimensional FEM simulation has been carried out to determine flux pattern, working flux density, force etc. for three-coil and four-coil based AMB utilizing ANSYS (version 12.1) which based on magnetic scalar potential. Detailed electromagnetic analysis on typical industrial AMB system has been performed and a comparative study between three and four coil based AMB has been carried out under different operating conditions. Extensive simulation has been conducted for both AMB's with varying parameters and a comparative study has been achieved in terms of electromagnetic properties. It is interesting to note that the flux, flux-density and force (both in nodal and vector plot) is more for 3-coil AMB than 4-coil AMB under similar operating conditions.

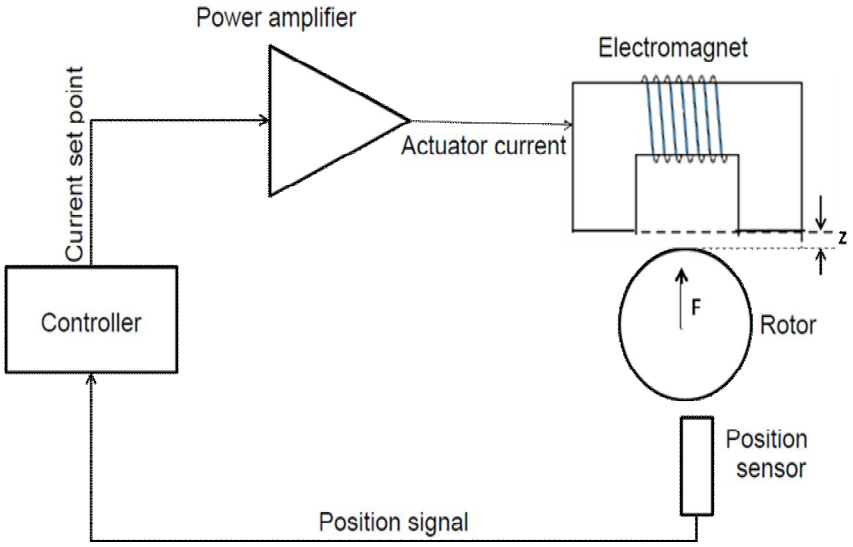

Figure 1. Basic block diagram of the active magnetic bearing

2. Flux density and force of magnetic circuit used in AMB

T Ampere circuital law which is integral form may be stated as

$$\oint_l H.dl = Ni \tag{1}$$

Where i is the current of the coil, N is the number of turns in the coil and H is the magnetic field intensity produced in the ferromagnetic core of the magnet by the current and *l* is the path enclosing a surface through which current flows [3].

$$Hl = Ni \quad \text{or} \quad H = \frac{Ni}{l} \tag{2}$$

$$B = \mu H \quad \text{or} \quad B = \frac{\mu Ni}{l} \tag{3}$$

This type of magnetic bearing is amenable to analysis via magnetic circuit theory. Assuming negligible leakage and fringing and neglecting the small reluctance of the iron parts of the flux path yield the following magnetic circuit as shown (Figure 2 and Figure 3) represent an electric circuit with batteries (mmf) and resistors. The flux ϕ is replaced by the current through the coil, and the reluctance *R* also replaced by the resistance, there are magneto motive force (MMF) sources of strength Ni. In terms of the geometry of the bearing, the reluctance is

$$R = \frac{2z}{\mu_0 A} \tag{4}$$

where z is the nominal air gap between the rotor and the pole face of the magnet of the bearing, A is the cross-sectional area of each leg, and μ_o is the permeability of free space ($4\pi X10^{-7}$ Tesla*Meter/Amp). The flux in the circuit may be represented as follows [3].

$$\phi = \oint_s B.ds = \frac{Ni}{R} = \frac{\mu_0 ANi}{2z} \tag{5}$$

The flux density, B is given below

$$B = \frac{\phi}{A} = \frac{\mu_0 Ni}{2z} \tag{6}$$

The main goal of the AMB is to produce desired electromagnetic forces to levitate the ferromagnetic rotor (shaft) located in the bearing. The electromagnetic force generated by the electromagnet is the gradient of the magnetic field energy and depends on the air gap size [9].

$$F = -\frac{dW}{dz} \tag{7}$$

And

$$W = \frac{1}{2}\int BHdV = \frac{1}{2}\oint_v \frac{B^2}{\mu_0} dV \tag{8}$$

Where F is the electromagnetic force, W is the magnetic field energy, and V is the air gap volume. The electromagnetic force is a nonlinear function of the coil current and the distance between the shaft and the electromagnet. The control algorithm produces electromagnetic force acting on the shaft using the power interface and electromagnet coil [3, 9].

$$F = \frac{B^2 A}{\mu_0} \tag{9}$$

Substituting in the expression determined for B yields:

$$F = \frac{\mu_0 A N^2 i^2}{z^2} \tag{10}$$

and the inductance of electromagnet

$$L = \frac{N\phi}{i} = \frac{N^2 \mu_0 A}{2z} \tag{11}$$

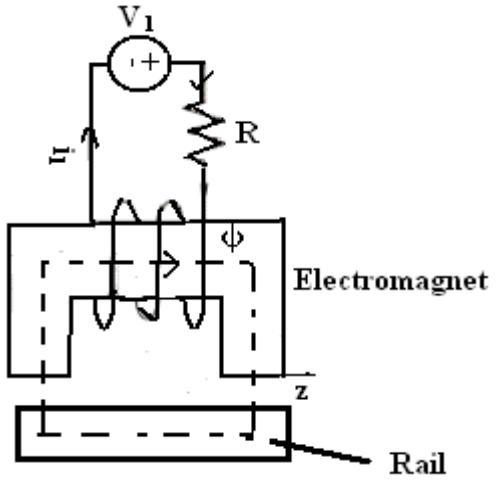

Figure 2. U-I type structure used for AMB

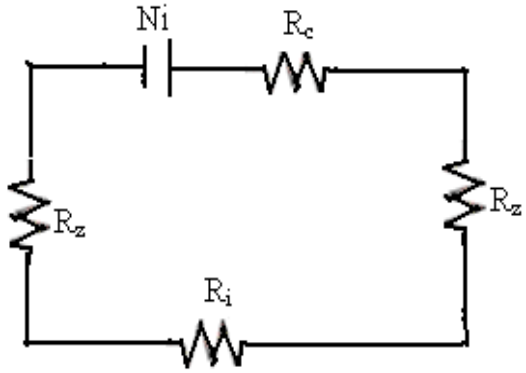

Figure 3. Magnetic circuit analysis

3. The FEM model of AMB

The magnetic field of the active magnetic bearing is analysed by finite element method (FEM). The magnetic field is assumed to be two dimensional and stationary. The calculation of forces and fields in active magnetic bearing is based on Maxwell's equations of electromagnetism. For general quasi-static fields these equations in the differential form can be written according to as [9, 10].

$$\nabla XH = J \tag{12}$$

$$\nabla XE = -\frac{\partial B}{\partial t} \tag{13}$$

$$\nabla .B = 0 \tag{14}$$

$$\nabla .J = 0 \tag{15}$$

$$\nabla .D = \rho_v \tag{16}$$

$$H = \frac{B}{\mu} \tag{17}$$

where H, B, J, D, ρ_v and μ are the magnetic field intensity, the magnetic flux density, the source current density, electric flux density, electric charge density and the permeability, respectively. The permeability is supposed to be constant, $\mu = \mu_0$ in air, and the relationship [9].

$$B = \mu_0 \mu_r (H + M) = \mu (H + M) \tag{18}$$

is used, where M is the magnetization vector, μ is the material permeability, μ_0 is the permeability of vacuum, and μ_r is the relative permeability of the material.

The equations (9), (10) and (12) are referred to as Maxwell-Ampere's law, Faraday's law and the equation of continuity respectively. The electric and magnetic forms of Gauss's law are described by the equation (11) and (13) respectively. To obtain a closed system the constitutive relations has to be included [9].

$$B = \mu H \tag{19}$$

$$D = \varepsilon E \tag{20}$$

$$\mathrm{J} = \sigma(\mathrm{E} + \mathrm{vXB}) + \mathrm{J}_1 \tag{21}$$

Where J_1, v, ε and σ are the external generated current, velocity of the conductor, permittivity and electrical conductivity, respectively.

Since the magnetic flux density is divergence free, there exists a magnetic vector potential A such that $B = \nabla XA$ which gives the potential formulation.

$$\nabla X(\frac{1}{\mu}\nabla XA - M) = J \tag{22}$$

In the finite element formulation of electromagnetic field problems, magnetic potential A is used in the solution of 2-D magnetic fields. The magnetic flux density and electric field intensity are given by the equalities as [9, 10].

$$B = \nabla XA \quad \text{and} \quad E = -\nabla v - \frac{\partial A}{\partial t} \tag{23}$$

where v is the electric scalar potential.

Using the magnetic vector potential and the constitutive relation in (1) leads to the linear partial differential equation

$$\nabla XH = \mu J \tag{24}$$

The magnetic vector potentials have been represented by first order vector shape functions which divergence is equal to zero, and it is resulting divergence-free magnetic vector potential (Coulomb gauge),

$$\nabla .A = 0 \tag{25}$$

It is supposed that the normal component of the magnetic flux density vanishes on the boundary, which cans be prescribed by the boundary condition [8, 9]

$$A \times n = 0 \tag{26}$$

The designed construction of the AMB consists of rotor and stators with coils. The heteropolar construction of the AMB consists of three and four pole-pairs at 120 and 90 degrees apart from each and other respectively (Figure 4). The following parameters: no of pole pairs -4, maximal radial air gap-(0.25-1)cm, rotor outer radius -50mm, no of coil turns-(500-800),current range-(0-6) A are considered for finite element analysis using ANSYS software.

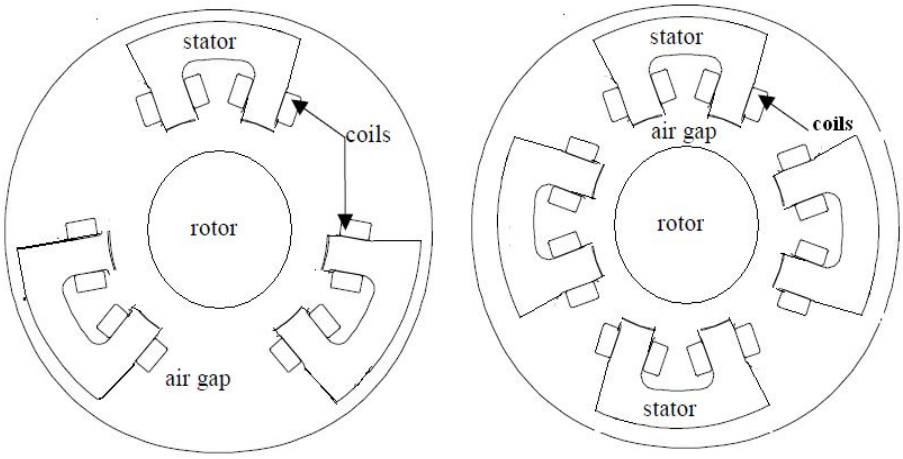

Figure 4. Three and four coil AMB construction

4. ANSYS software simulation for three and four coil AMB

ANSYS Multiphysics is a powerful interactive environment for modeling and solving all kinds of scientific and engineering problems based on partial differential equations (PDEs). To solve the PDEs, ANSYS Multiphysics uses the proven finite element method (FEM) [7]. The software runs the finite element analysis together with adaptive meshing and error control using a variety of numerical solvers. The user can perform a various types of analysis including stationary and time dependent analysis, linear and nonlinear analysis, eigen frequency and modal analysis. This paper is focused on a two-dimensional magneto static analysis of the three and four coil AMB.

(Figure 5) represent as flow chart of calculation of flux pattern and force by using ANSYS

software for AMB 4-coil structure. In the 2D mode, the shapes are partitioned into triangles. The sides of the triangles are called mesh edges, and their corners are mesh vertices. A mesh edge must not contain mesh vertices in its interior [7]. Similarly, the boundaries defined in the geometry are partitioned (approximately) into mesh edges, the so-called boundary elements, which have to conform to the triangles if there is an adjacent sub domain. For a defined mesh, a set of approximations to the dependent variables is introduced. A function approximating a variable is defined by a finite number of parameters (called the degrees of freedom, DOFs). This approximation is used in a weak form of an equation and a set of DOF system equations is given.

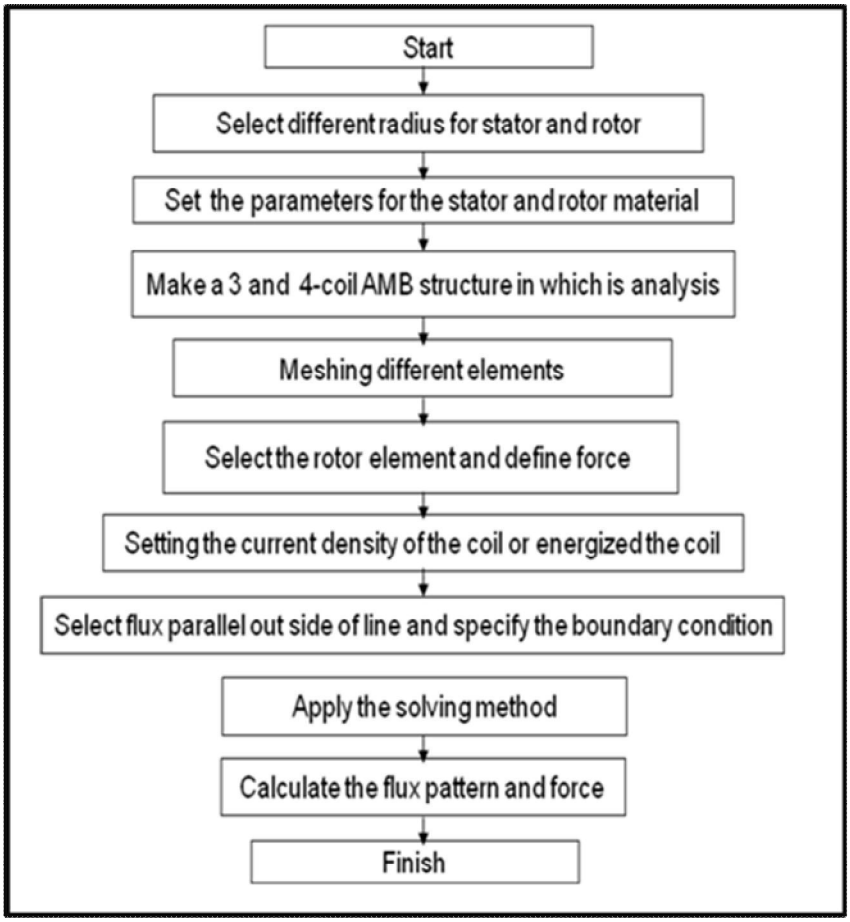

Figure 5. Flow chart of calculation of flux pattern and force by using ANSYS software for AMB 3 and 4-coil structure

5. Simulation results and discussion

Two-dimensional FEM simulation has been carried out to determine flux pattern, working flux density, force etc. for three and four coil AMB. Commercial FEM software ANSYS (version 12.1) has been used for this purpose. The flux pattern of 3-coil and 4-coil AMB with air-gap of 0.5 cm and coil-current of 6A utilizing two different turns (500 and 700) are shown in Figure 6 to Figure 9 respectively. Figure 10 to Figure 11 shows vector plot of flux density respectively for 3-coil and 4 coil based AMB with air-gap of 0.5 cm, coil-current of 6A and no of turns 500. Figure 12 and Figure 13 shows vector plot of force for the above system using same parameters. Different simulation has been carried out for different air-gap position. It has been noticed that

with the increase of air-gap, leakage flux is increased and the flux linkage between magnet (stator) and rotor is decreased. As expected, the vector plot of flux density and force of three and four coil AMB are decreased with the increase of the air gap between magnet (stator) and rotor (Figure 10 to Figure 13). The generated flux, flux density and force are increased with increase of number of turns of coil and decreased with increase of air gap at the same coil-current (6A) for 3-coil and 4-coil AMB. Figure 14 to Figure 16 represents the characteristic of flux, flux density and force for 3-coil and 4-coil AMB utilizing same number of turns and coil-current. It has been observed the generated flux, flux density and force are decreased with the increase of air-gap and vice-versa. It is interesting to note that the flux, flux-density and force (both in nodal and vector plot) is more for 3-coil AMB than 4-coil AMB irrespective of any operating air-gap position. It is obvious that the cross-coupling phenomenon is more in 4-coil AMB than 3-coil AMB. Due to more no of actuators, interactions between the generated fluxes are more in 4-coil AMB. Again possibility of induced eddy currents is more in 4-coil AMB than 3-coil AMB. The flux produced by these eddy currents will oppose the main flux. As expected reduction of main flux as well as Maxwell tensor force is more in 4-coil AMB.In the above cases it is assumed to have fixed coil-current irrespective of any air-gap and the simulation is carried out with different air-gap positions. But in real time operation with increase of operating air-gap the required current for levitation will be more. Figure 17 and Figure 18 represents the characteristic of flux and force for 3-coil and 4-coil AMB utilizing different number of turns and same coil-current. It has been noticed that the generated flux and force are increased with the increase of number of turns and vice-versa. Figure 19 to Figure 20 represents the 3-D plot for flux, and force respectively of 3-coil and 4-coil AMB with different air-gap and corresponding coil-current. It is apparent that with the increase of air-gap the required coil-current increases and correspondingly the generated field flux and Maxwell tensor force increases and vice-versa.

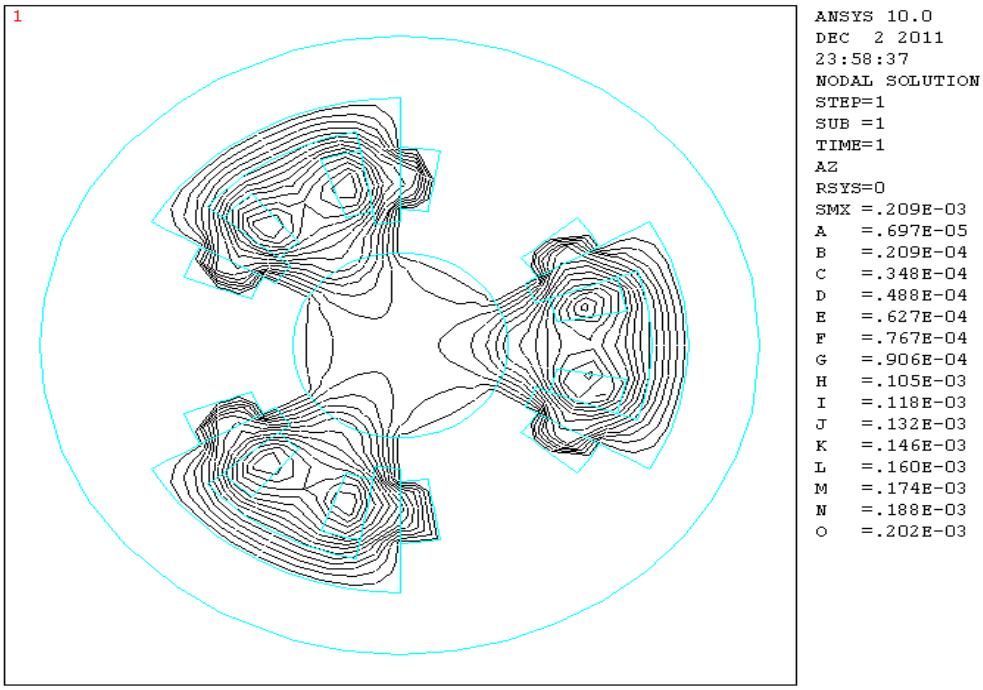

Figure 6. Flux pattern of 3-coil AMB for z=0.5 cm, i=6A and N=500

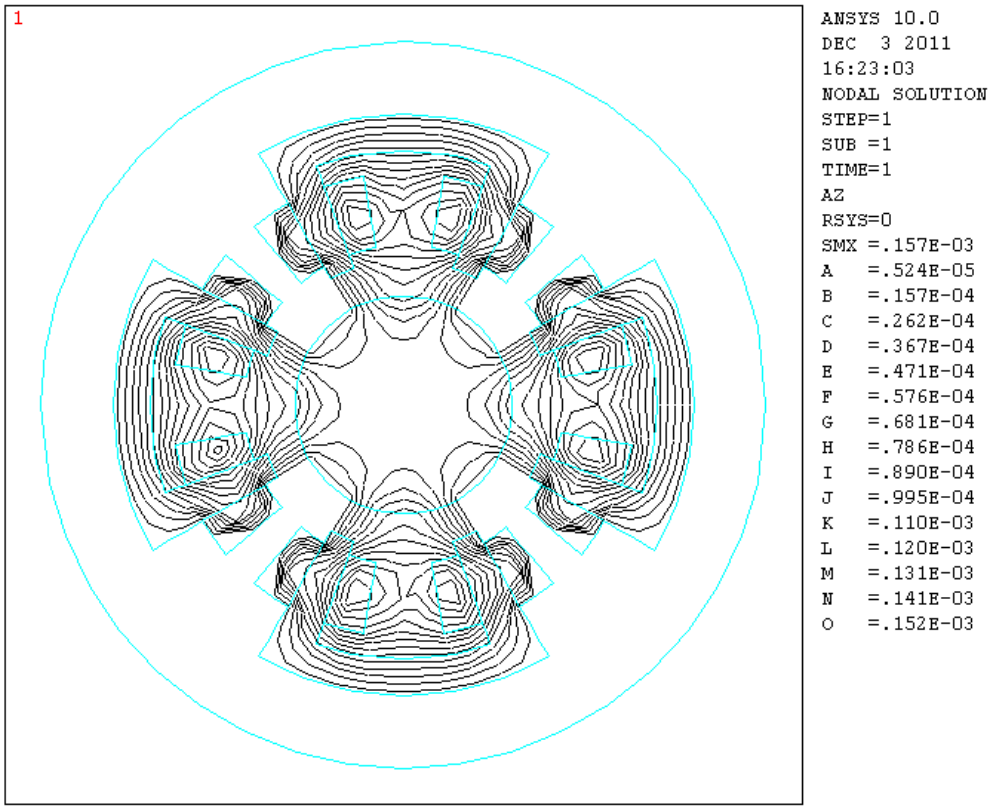

Figure 7. Flux pattern of 4-coil AMB for z=0.5 cm, i=6A and N=500

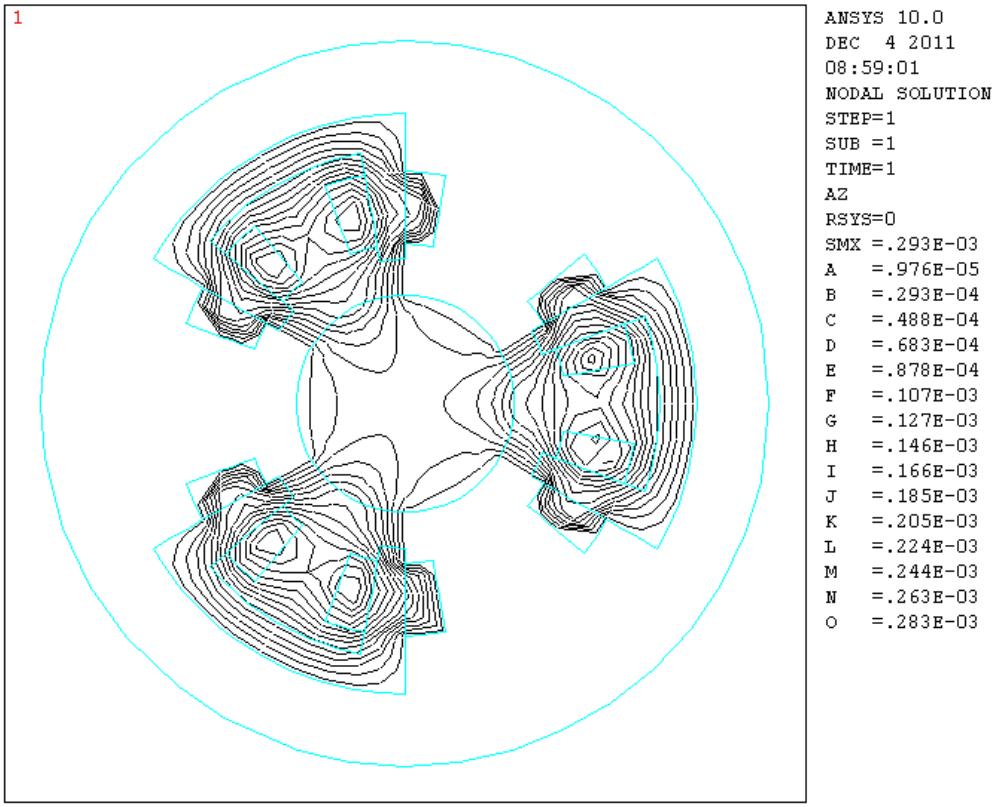

Figure 8. Flux pattern of 3-coil AMB for z=0.5 cm, i=6A and N=700

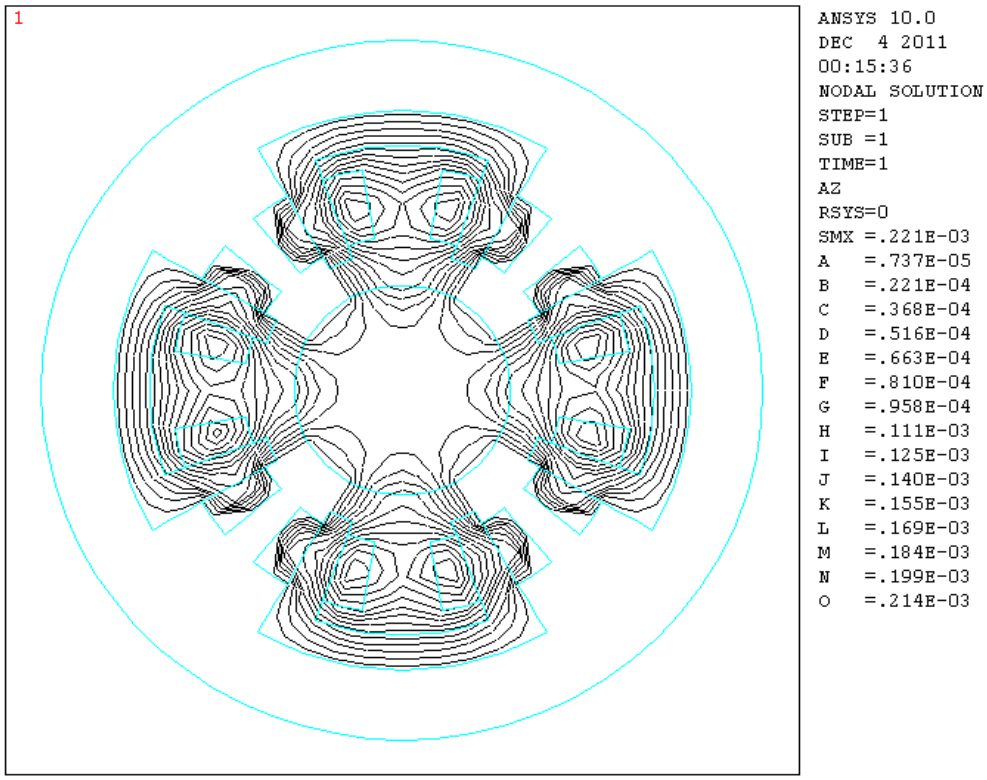

Figure 9. Flux pattern of 4-coil AMB for z=0.5 cm, i=6A and N=700

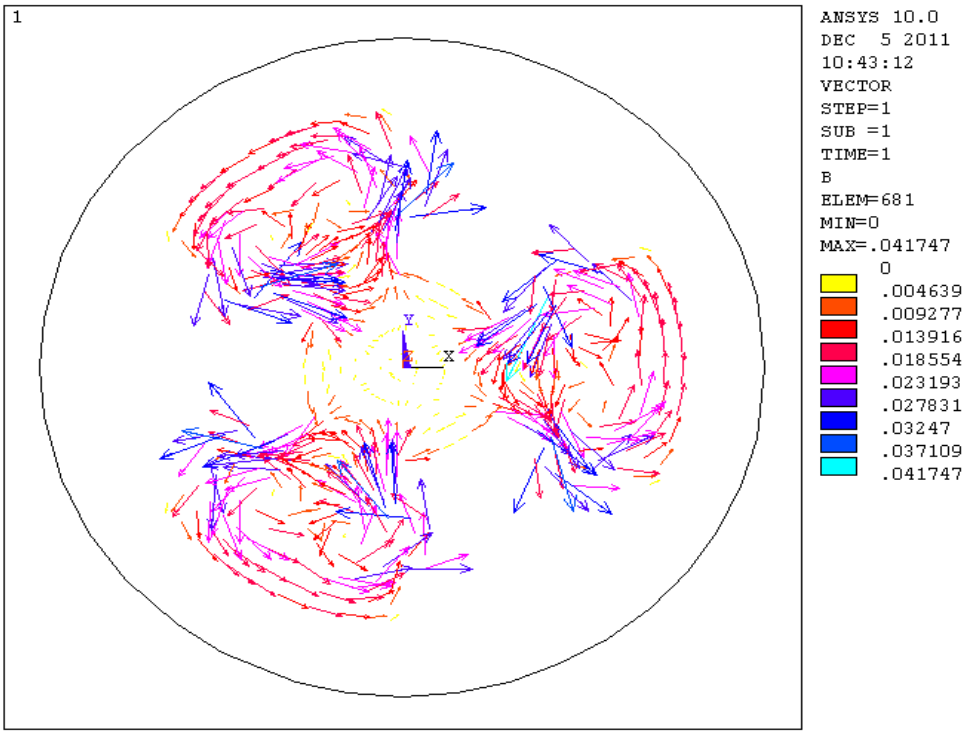

Figure 10. Vector plot of flux density of 3-coil AMB for z=0.5 cm, i=6A and N=500

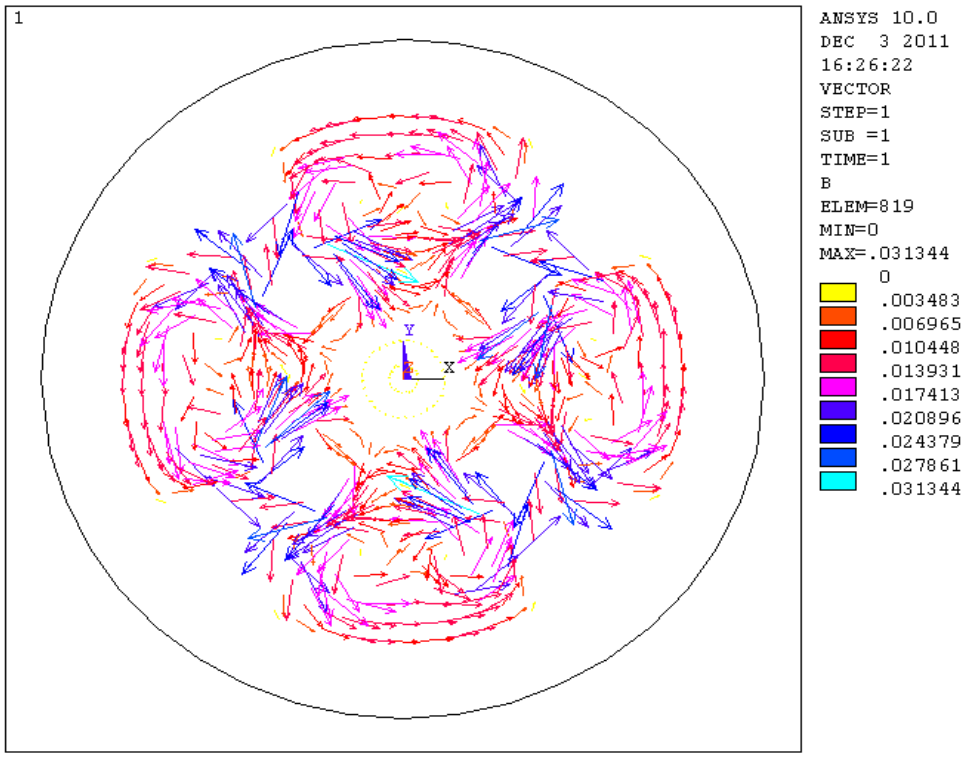

Figure 11. Vector plot of flux density of 4-coil AMB for z=0.5 cm, i=6A and N=500

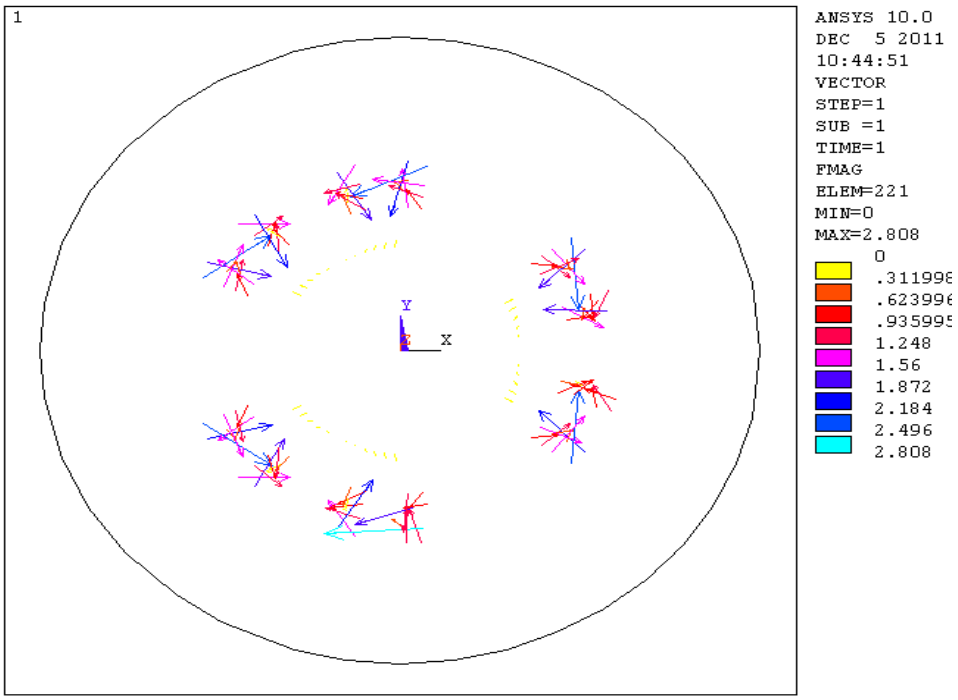

Figure 12. Vector plot of force of 3-coil and 4-coil AMB for z=0.5 cm, i=6A and N=500

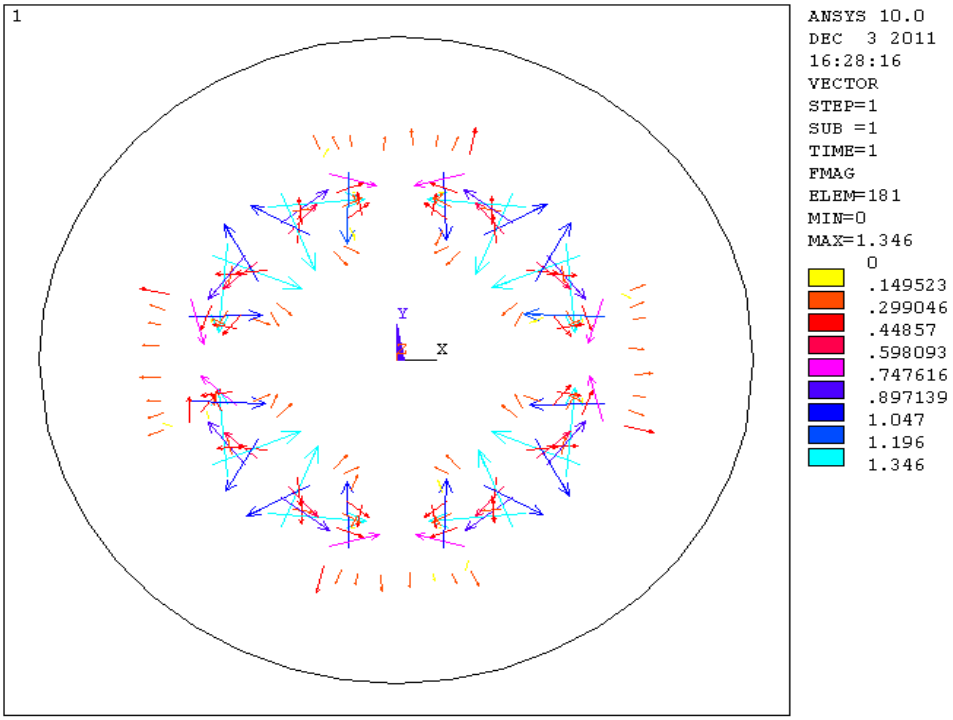

Figure 13. Vector plot of force of 3-coil and 4-coil AMB for z=0.5 cm, i=6A and N=500

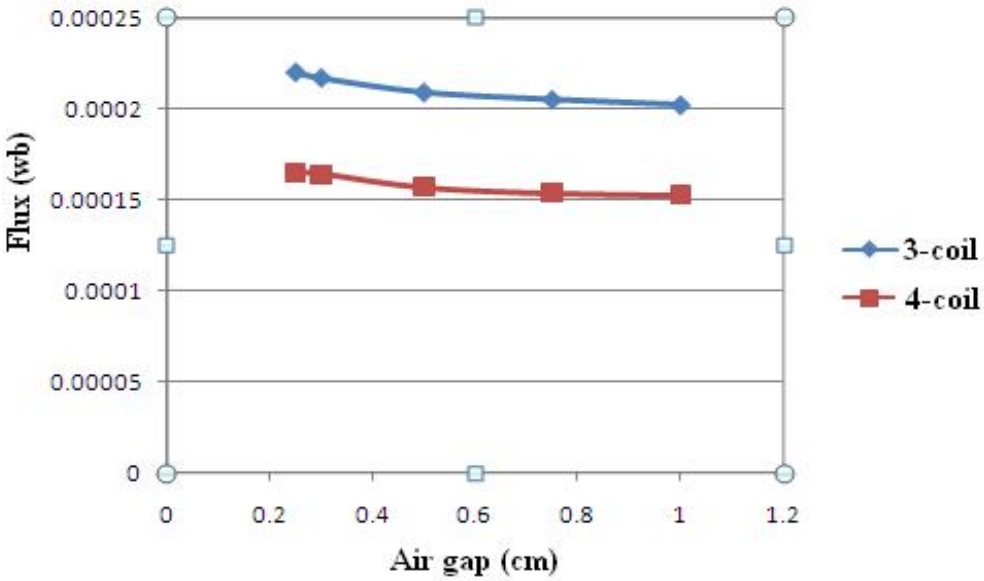

Figure 14. Flux vs. air gap for i=6A and N=500 of 3-coil and 4-coil AMB

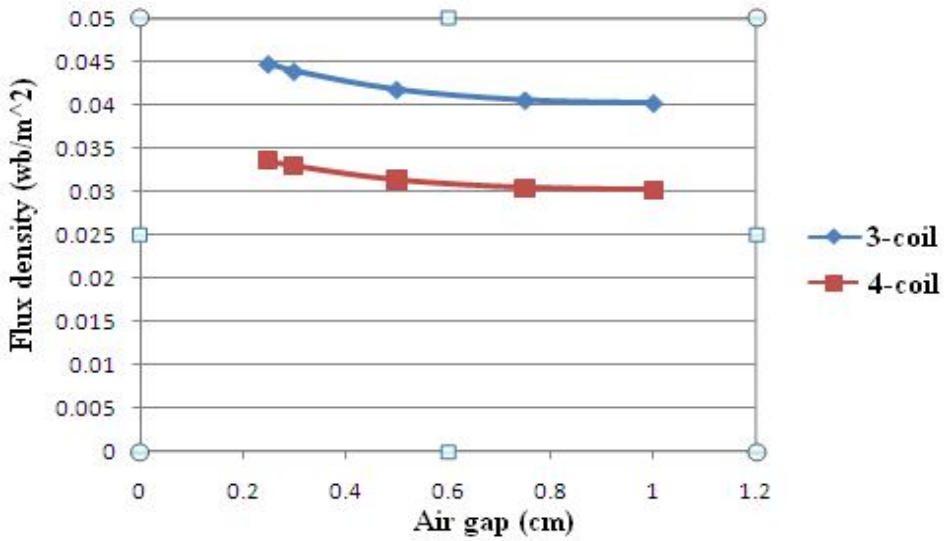

Figure 15. Flux density vs. air gap for i=6A and N=500 of 3-coil and 4-coil AMB

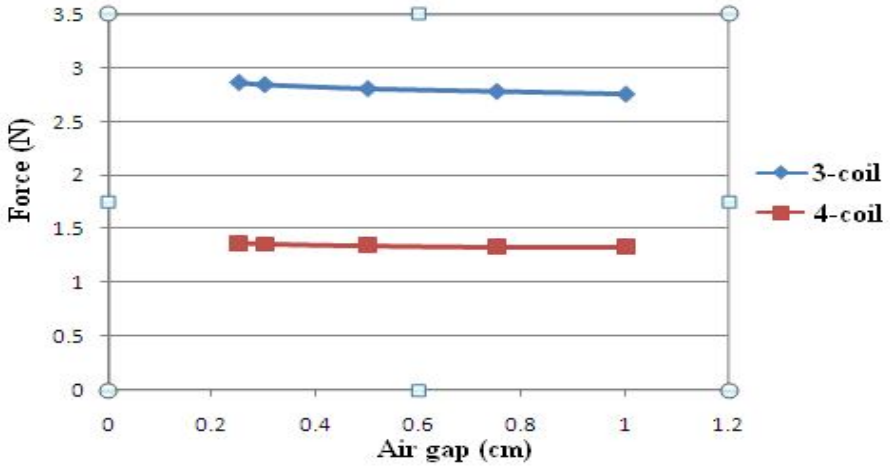

Figure 16. Maxwell's tensor force vs. air gap for i=6A and N=500 of 3-coil and 4- coil AMB

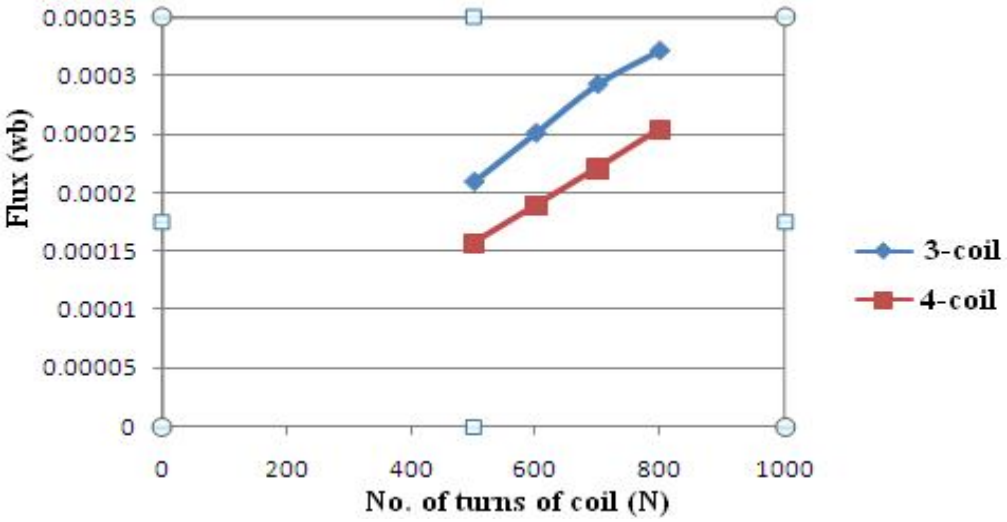

Figure 17. Flux vs. no. of turns for i=6A and air-gap=0.5 cm of 3-coil and 4-coil AMB

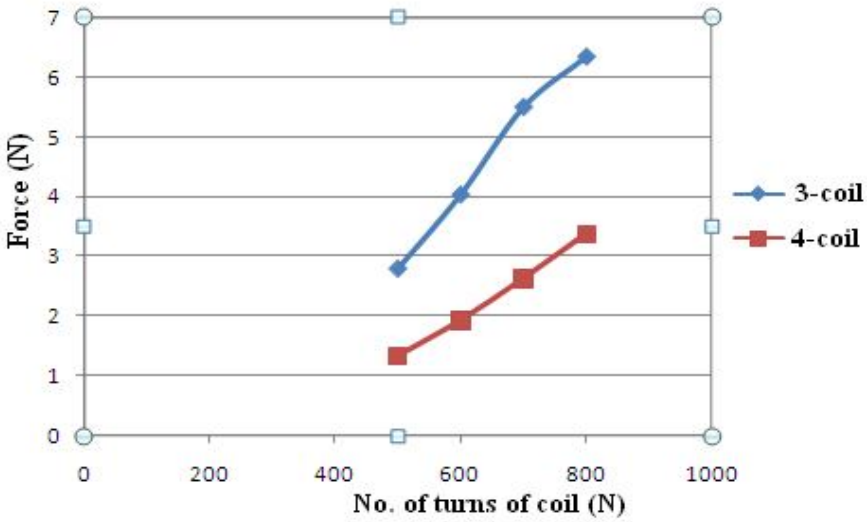

Figure 18. Force vs. no. of turns for i=6A and air-gap=0.5 cm of 3-coil and 4-coil AMB

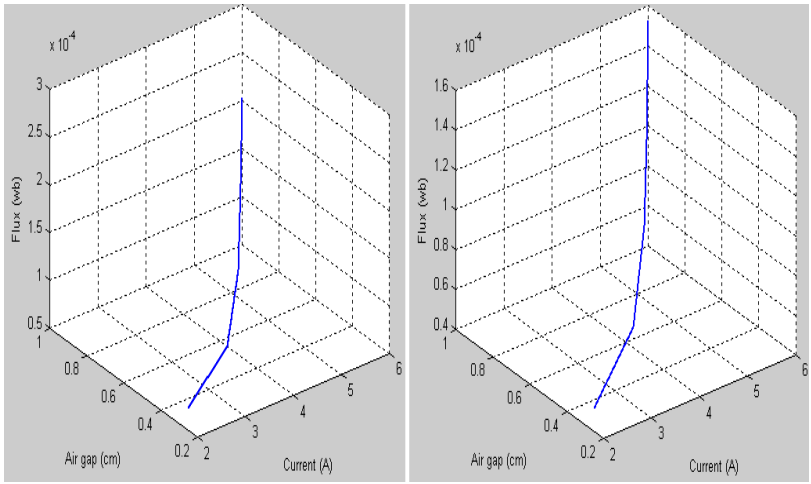

Figure 19. 3-D plot of flux, air gap and current for 3-coil (left) and 4-coil (right) AMB

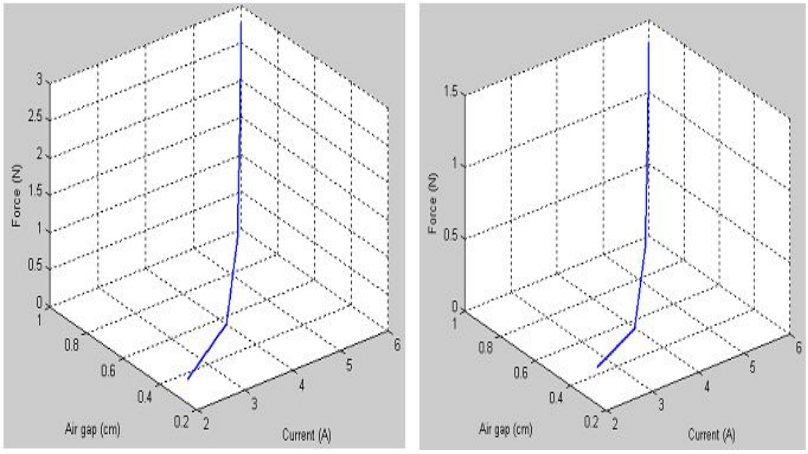

Figure 20. 3-D plot of force, air gap and current for 3-coil (left) and 4-coil (right) AMB

6. Conclusion

This work is focused on 2D and 3D modeling and analysis using the electromagnetic module with ANSYS software to examine the static AMB behavior in the real operation environment. In this paper ANSYS Based FEM analysis has been performed for three and four coil based active magnetic bearing. A comparative study of three and four coil AMB has been presented. Comparative results of ANSYS simulation of three and four coil AMB has also been presented for different air- gap and coil-current. It is concluded that the simulated results of 3-coil AMB is superior to 4-coil AMB the flux and force are determined by FEM-based analysis using the Maxwell's stress tensor and virtual work. It is essential to use appropriate materials for the rotor and stator.

Acknowledgments

The author wishes to acknowledge DST, Govt. of India for sponsoring the Project No.SR/S3/EECE/0008/2010 entitled "Development of DC Electromagnetic Levitation Systems-Suitable for Specific Industrial Applications".

References

[1] Piłat, A. 2004. FEMLab software applied to active magnetic bearing analysis, *International Journal of Applied Mathematics and Computer Science*. Spec. iss.: Issues in modeling, optimization and controls, 14, 4: 497-501.
[2] Piłat, A. 2006. *Selected magnetostatic analysis of 3-coil Active Magnetic Bearing, expert from the proceeding of the COSMOL Users conference*, Prague.
[3] Meeker, D. 1999. Example: Radial Magnetic Bearing (Nonlinear Magneto static,), http://femm.fostermiller. Net/wiki/Examples.
[4] Ludvig, T. and Kuczmann, M. 2008. Design of active magnetic bearing. *Journal of optoelectronics and advanced materials*, 10, 7: 1834-1836.
[5] Gosiewski, Z. and Falkowski, K. 2003. "*Multifunction magnetic bearings"*. Biblioteka Naukowa Institute Lotnictwa, Warszawa (in Polish).
[6] Ohmori, K., Kim, S., Masuzawa, T., and Okada, Y. 2002. Design of an Axial-type Self Bearing Motor for Small Axial Pump. *Proceedings of The Eighth International Symposium on Magnetic Bearings*, Japan, August 26-28.
[7] Maslen, E. 1999. Magnetic Bearings, Charlottesville, Virginia, USA, (personal note).
[8] Reference Guide ANSYS CFX-Solver, Release 12.1.
[9] Mathew, N.O. 2009. "*Sadiku, Element of Electromagnetic*". OXFORD University press.
[10] Rothwell, E. J. and Cloud, M. J. 2001. "*Electromagnetics*". CRC Press.
[11] Hammond, P. and Sykulski, J. K. 1994. "*Engineering Electromagnetism-Physical Processes and Computation*". Oxford University Press, New York.
[12] Pahner, U., Mertens, R., De Gersem, H., Belmans, R., and Hameyer, K. 1998. A parametric finite element environment tuned for numerical optimization. *IEEE Transactions on Magnetics*, 34, 5: 2936-2939.
[13] Gorazd ˇStumberger, Drago Dolinar, Uwe Pahner, and Kay Hameyer. 2000. Optimization of Radial Active Magnetic Bearings Using the Finite Element Technique and the Differential Evolution Algorithm. *IEEE Transactions on Magnetics*, 36, 4: 1009-1013.
[14] Antila, M., Lantto, E., and Arkkio, A. 1998. Determination of forces and linearized

parameters of radial active magnetic bearings by finite element technique. *IEEE Transaction on Magnetics*, 34, 3: 684-694.
[15] Hantila, I. F. 1975. A Method For Solving Stationary Magnetic Field in Nonlinear Media. *Rev. Roum. Sei. Techn. Electrotechn. Et. Energ,* 20, 397.
[16] Hsu, C. T. and Chen, S. L. 2002. Exact Linearization of a Voltage-Controlled 3-Pole Active Magnetic Bearing System. *IEEE Transactions on Control Systems Technology*, 10, 4: 618-625.
[17] Schweitzer, G. 2002. Active magnetic bearings-chances and limitation. *International Centre for Magnetic Bearings, ETH Zurich*, CH-8092 Zurich.
[18] Mukhopadhyay, S. C., Ohji, T., Iwahara, M., and Yamada, S. 1999. Design, analysis and control of a new repulsive type magnetic bearing. *IEE proc. on Elect. Pwr. Appl.* 146, 1: 33-40, Jan.
[19] Polazer, B., Stumberger, G., Ritonia, J., and Dolinar, D. 2008. Variations of active magnetic bearing linearized model parameters analyzed by finite element computation. *IEEE Transaction on Magnetics*, 44, 6: 1534-1537.